Author Manuscript

Author Manuscript

Author Manuscript

Author Manuscript

HHS Public Access

Author manuscript

J Autoimmun. Author manuscript; available in PMC 2017 May 01.

Published in final edited form as:

J Autoimmun. 2016 May ; 69: 86–93. doi:10.1016/j.jaut.2016.03.004.

Nanovesicle-targeted Kv1.3 knockdown in memory T cells suppresses CD40L expression and memory phenotype

Ameet A. Chimote[1], **Peter Hajdu**[1], **Leah C. Kottyan**[2], **John B. Harley**[2,4], **Yeoheung Yun**[3], and **Laura Conforti**[1,*]

[1]Department of Internal Medicine, Division of Nephrology, University of Cincinnati, Cincinnati OH

[2]Center for Autoimmune Genomics and Etiology, Cincinnati Children's Hospital Medical Center, University of Cincinnati College of Medicine, Cincinnati, Ohio

[3]North Carolina A & T State University, Chemical, Biological and Bioengineering Department, Greensboro, NC

[4]US Department of Veterans Affairs Medical Center, Cincinnati, OH

Abstract

Ca^{2+} signaling controls activation and effector functions of T lymphocytes. Ca^{2+} levels also regulate NFAT activation and CD40 ligand (CD40L) expression in T cells. CD40L in activated memory T cells binds to its cognate receptor, CD40, on other cell types resulting in the production of antibodies and pro-inflammatory mediators. The CD40L/CD40 interaction is implicated in the pathogenesis of autoimmune disorders and CD40L is widely recognized as a therapeutic target. Ca^{2+} signaling in T cells is regulated by Kv1.3 channels. We have developed lipid nanoparticles that deliver Kv1.3 siRNAs (Kv1.3-NPs) selectively to $CD45RO^{+}$ memory T cells and reduce the activation-induced Ca^{2+} influx. Herein we report that Kv1.3-NPs reduced NFAT activation and CD40L expression exclusively in $CD45RO^{+}$ T cells. Furthermore, Kv1.3-NPs suppressed cytokine release and induced a phenotype switch of T cells from predominantly memory to naïve. These findings indicate that Kv1.3-NPs operate as targeted immune suppressive agents with promising therapeutic potentials.

Keywords

Autoimmunity; T cell; Kv1.3 ion channel; CD40 ligand; Lipid nanoparticles; Ca^{2+} signaling

*Corresponding author: Dr. Laura Conforti, Department of Internal Medicine, Division of Nephrology, University of Cincinnati, 231 Albert Sabin Way, Cincinnati, OH 45267-0585. Fax (513) 558-4309; Phone (513) 558-6009; Laura.Conforti@uc.edu.

COMPETING INTERESTS

The authors do not have any competing interests.

Publisher's Disclaimer: This is a PDF file of an unedited manuscript that has been accepted for publication. As a service to our customers we are providing this early version of the manuscript. The manuscript will undergo copyediting, typesetting, and review of the resulting proof before it is published in its final citable form. Please note that during the production process errors may be discovered which could affect the content, and all legal disclaimers that apply to the journal pertain.

Author Manuscript Author Manuscript Author Manuscript Author Manuscript

1. INTRODUCTION

The activity of T lymphocytes relies on Ca^{2+} signaling which regulates cytokine production and expression of co-stimulatory molecules necessary for stimulation of B cells, macrophages and dendritic cells (DC) [1]. Defects in Ca^{2+} signaling have been reported in autoimmune diseases including inflammatory bowel disease (IBD), rheumatoid arthritis (RA) and systemic lupus erythematosus (SLE) [1–5]. Particularly in SLE, the overactive T cells show increased nuclear factor of activated T cells (NFAT) nuclear translocation [6, 7] and overexpression of CD40L (CD154), which binds CD40 in B cells and leads to increased B cell activation and, consequently, inflammatory cytokine release, autoantibody formation and disease progression [1, 8–12]. Moreover, CD40L activates DCs causing them to release B cell activation factor (BAFF) that promotes B cell survival and further autoantibody production [11, 13, 14]. This crosstalk between hyperactive T cells, B cells and DCs, which is accentuated by CD40L overexpression, constitutes a vicious circle in SLE patients, and ultimately leads to disease flare and end-stage organ damage. Enhanced T cell receptor (TCR)-mediated Ca^{2+} influx and CD40L expression have also been reported in IBD and contribute to the development of the disease [5, 15].

Ca^{2+} signaling in T cells is controlled by ion channels which regulate Ca^{2+} influx into the cells. Specifically, T lymphocyte activation is initiated by TCR engagement which results in the influx of Ca^{2+} through Ca^{2+}-release activated Ca^{2+} (CRAC) channels [16, 17]. The consequent increase in intracellular Ca^{2+} levels ($[Ca^{2+}]_i$) activates calcineurin, a calmodulin-dependent serine-threonine phosphatase, which, in turn, dephosphorylates and activates NFAT [6, 16–19]. The sustained influx of Ca^{2+} necessary for NFAT activation is guaranteed by K^+ channels, Kv1.3 and KCa3.1, which maintain the negative membrane potential thus providing the electrochemical driving force for Ca^{2+} influx through CRAC channels. Kv1.3 channels in particular are highly expressed in effector memory T cells and control their activity [20–22]. Inhibition of Kv1.3 by pharmacological blockers inhibits the Ca^{2+} response to antigen stimulation and ameliorates autoimmune diseases such as psoriasis and multiple sclerosis (MS) in animal models [23, 24].

The transcription of CD40L is Ca^{2+} and NFAT dependent [6]. Thus, a therapeutic approach that suppresses Ca^{2+} influx and CD40L expression in memory T cells may be advantageous over available immunosuppressive drugs targeting the CD40/CD40L system [12]. The ability to control CD40L in memory T cells is particularly attractive as autoantigen-specific memory T lymphocytes guarantee the life-long preservation of immune memory in autoimmune diseases and long-lived active B cells. Attempts were made to suppress CD40L in T cells using anti-CD40L antibodies, and indeed these antibodies were effective in treating SLE, RA, MS and IBD in animal models; however, the risk of thrombocytopenia (CD40L is expressed on platelets) halted phase 2 clinical trials [2, 11, 25].

Our laboratory has developed functionalized lipid nanoparticles (NPs) that can deliver siRNAs against Kv1.3 channels (Kv1.3-NPs) selectively to $CD45RO^+$ T cells and has demonstrated that these NPs can effectively knock down Kv1.3 channels and suppress Ca^{2+} influx in $CD45RO^+$ memory T cells [26]. The current study was undertaken to determine

Author Manuscript Author Manuscript Author Manuscript Author Manuscript

whether these Kv1.3-NPs are effective in controlling CD40L expression in CD45RO$^+$ T cells.

2. MATERIALS AND METHODS

2.1 Human subjects

Blood samples were obtained from either healthy volunteers or blood bank donors (unused blood units from the Hoxworth Blood Bank Center, Cincinnati, OH). The healthy volunteers were Caucasian females in the age range of 36–56 years. Studies and informed consent forms were approved by the University of Cincinnati.

2.2 Cell culture reagents

Human serum was obtained from Sigma-Aldrich (St. Louis, MO). For cell culture, HEPES, RPMI-1640, penicillin, and streptomycin were obtained from Thermo Fisher Scientific Inc (Waltham, MA), while L-glutamine was obtained from Sigma-Aldrich.

2.3 Cell isolation

PBMCs were isolated from whole blood using Ficoll-Paque (GE Healthcare Bio-sciences AB, Uppsala, Sweden) density gradient centrifugation. CD3$^+$ cells were separated by negative selection from PBMCs using the EasySep™ Human T cell Enrichment Kit (Stem Cell Technologies, Vancouver, BC, Canada) according to the manufacturer's instructions. Memory CD4$^+$ T cells were separated by negative selection from PBMCs using the EasySep™ Human Memory CD4$^+$ T cell Enrichment Kit (Stem Cell Technologies) according to the manufacturer's instructions. T cells were maintained in RPMI-1640 medium supplemented with 10% human serum, 200 u/ml penicillin, 200 μg/ml streptomycin, 1 mM L-glutamine. For the experiments that were performed to determine intracellular staining of IFN-γ and TNF-α, memory CD4$^+$ T cells were maintained in RPMI-1640 supplemented with 2% human serum, 200 u/ml penicillin, 200 μg/ml streptomycin, 1 mM L-glutamine.

2.4 Nanoparticle (NP) preparation

NPs were prepared and functionalized as previously described by us [26]. Briefly, lipid vesicles composed of L-α-phosphatidylcholine (PC), 1,2-distearoyl-sn-glycero-3-phosphoethanolamine-N-[biotinyl(polyethylene glycol)-2000] (PE-PEG-biotin) and cholesterol (CH) (Avanti Polar Lipids Inc., Alabaster, AL) were obtained by mixing the chloroform solutions of each lipid at a 3:1:1 mole ratio, drying them with N_2, rehydrating them with PBS (pH = 7.4), and maintaining them in an incubator in a shaker at 37°C for 2 hours. Unilamellar nanovesicles of 100 nm diameter were then obtained by sonication and extrusion (LIPEX™ Thermobarrel Extruder, Northern Lipids Inc., Burnaby, BC, Canada). The size of the NPs was confirmed with Zetasizer Nano ZS (Malvern Instruments Inc, Westborough, MA). The NPs were then functionalized to selectively recognize CD45RO$^+$ T cells by attaching Alexa 647 or Alexa 488 conjugated streptavidin (SAV, Biolegend, San Diego, CA) and biotinylated anti-human CD45RO antibody (Clone: UCHL1 10 μg/ml, Biolegend, Cat #304220) on the surface of the NPs. The unbound antibody and SAV were removed by CL-4B columns (GE Healthcare Bio- Sciences AB). Prior to siRNA

Author Manuscript Author Manuscript Author Manuscript Author Manuscript

encapsulation, the NPs were frozen at −80°C for 2–4 h and then lyophilized for 48 h. 50 μg of the lyophilized NPs were reconstituted in 100 μl of nuclease-free water that contained 200–400 pM of either Kv1.3 siRNA (Santa-Cruz Biotechnology Inc., Dallas, TX, Cat # sc-42712, Kv1.3-NPs) or non-targeting scramble sequence siRNA (Santa-Cruz Biotechnology, Cat # sc-37007, scr-NPs) with protamine sulfate (Sigma Aldrich) at 1:5 molar ratio. Reconstituted NPs without siRNAs were used as negative controls (null-NPs). 3 × 10^5 freshly isolated T cells were mixed with 50 μl of the Kv1.3-, scr- or null-NPs and maintained in T cell medium in a humidified incubator in the presence of 5% CO_2 at 37 °C for 24 h prior to activation.

2.5 Cell activation

T cells were activated using either 40.5 nM phorbol-12-myristate-13-acetate (PMA, EMD Millipore, Billerica, MA) supplemented by 1.5 μM ionomycin (Sigma-Aldrich), 2 μM thapsigargin (TG, Sigma-Aldrich) or 10 μg/ml mouse anti-human CD3 antibody (BD Biosciences, San Jose, CA, Cat # 555336) along with 10 μg/ml mouse anti-human CD28 antibody (BD Biosciences, Cat # 555726). The activation times for each activation protocol are mentioned in the individual figure legends.

2.6 NFAT nuclear translocation

6 × 10^5 T cells were transduced with NPs that contained siRNA, activated with TG, surface-labeled with Alexa Fluor 647-CD45RO and then fixed in 1% paraformaldehyde solution (Affymetrix, Santa Clara, CA) and permeabilized in PBS containing 0.1% Triton X-100 (Sigma-Aldrich). NFAT staining was performed with Alexa Fluor 488 anti-NFATc1 antibody (25 μg/ml, Biolegend, Cat # 649604) as previously described [27]. Nuclei were stained with DAPI (100 nM, Life Technologies, Carlsbad, CA) just prior to sample acquisition. Samples were acquired on an ImageStream X Flow cytometer (Amnis Corporation, Seattle, WA) and the images were analyzed with IDEAS software (Amnis Corporation, Seattle, WA) as described in detail in Supplemental Fig S1. Briefly, only those cells that were positive for Alexa 647 fluorescence (cells that incorporated Alexa 647-CD45RO functionalized NPs) were recorded. In this population, single focused cells that were double positive for NFAT and DAPI signals were selected and nuclear localization of NFAT was quantitated as a similarity score, which represents the correlation of pixels in the selected individual cells for the DAPI and NFAT channels.

2.7 Cell surface antibody staining

Cell surface staining for CD40L, CD45RO and CD45RA was performed according to standard flow cytometry protocols. Briefly, 6 × 10^5 $CD3^+$ T cells were pre-incubated with NPs that were functionalized with Alexa Fluor 488-CD45RO antibody as described in section 2.4 and contained siRNA. Cells were then activated and stained for flow cytometry. For CD40L cells were stained live with Alexa Fluor 647 conjugated anti-CD40L antibody (Biolegend, Cat# 310818) according to the manufacturer's protocol, and fixed with 1% paraformaldehyde. For CD45RO and CD45RA staining, 2 × 10^5 cells out of the 6 × 10^5 NP-treated activated memory $CD4^+$ T cells were labeled live with 7-AAD viability staining solution (Biolegend, Cat # 420403) and analyzed immediately by flow cytometry. The remainder of the cells were labeled live with PE anti-CD45RO (Biolegend, Cat # 304206)

Author Manuscript Author Manuscript Author Manuscript Author Manuscript

and PB anti-CD45RA (Biolegend, Cat# 304123) antibodies and fixed with 1% paraformaldehyde. Data were collected on a LSR II cytometer (BD Biosciences, San Jose, CA) and analyzed using FlowJo software (FlowJo LLC, Ashland, OR). Gating strategies during FlowJo analysis for each flow cytometry experiment are described in detail in the figure legends.

2.8 Intracellular cytokine measurements

For intracellular staining of IFN-γ and TNF-α, 6×10^5 memory $CD4^+$ T cells were treated either scr- or Kv1.3-NPs and maintained overnight in T cell medium with 2% human serum as described above (Sections 2.3 and 2.4). Cells were then activated for 3 h with PMA/ionomycin in the presence of BD GolgiPlug Protein Transport Inhibitor (1 μl GolgiPlug/1 ml medium, BD Biosciences Cat#: 555029), fixed in 1% paraformaldehyde (Affymetrix), permeabilized with BD Perm/Wash buffer for 15 min and then stained for intracellular cytokines with APC-anti-IFN-γ (Biolegend, Cat#: 502511) and PerCP-anti-TNF-α (Biolegend, Cat#: 502923). Cells were then centrifuged and resuspended in cell staining buffer (Biolegend) and analyzed by flow cytometry (LSR II cytometer and FlowJo software).

2.9 Statistical Analysis

All data are presented as means ± SEM. Statistical analyses were performed using either Student *t*-test (paired or unpaired) or one-way ANOVA for differences across groups. Post hoc testing for the one-way ANOVA was determined by Holm-Sidak method. Statistical analysis was performed using SigmaPlot 13.0 (Systat Software Inc., San Jose, CA). p value < 0.05 was defined as significant.

3. RESULTS

3.1 Kv1.3 nanoparticles decrease NFAT nuclear translocation in memory T cells

T cell activation is accompanied by an increase in $[Ca^{2+}]_i$ which activates NFAT by mobilizing it to the nucleus to lead the transcription of CD40L and pro-inflammatory cytokines [6, 16, 17]. We have previously shown that the activation-induced increase in $[Ca^{2+}]_i$ in T cells is blocked by the treatment with Kv1.3-NPs that can selectively deliver siKv1.3 to $CD45RO^+$ T cells and knock down Kv1.3 channels [26]. Firstly, we performed experiments to determine whether the inhibition of $[Ca^{2+}]_i$ by Kv1.3-NPs is effectively reducing NFAT activation in memory T cells. NFAT activation was quantitated using imaging flow cytometry to measure the nuclear translocation of NFAT in T cells. T lymphocytes were incubated overnight with fluorescent CD45RO-NPs that incorporated either Kv1.3 siRNA (Kv1.3-NPs) or scramble sequence siRNA (scr-NPs). Also, nanoparticles that did not contain either Kv1.3 or scramble siRNA, but were coated with anti-CD45RO antibody, were included as controls for T cell activation (empty nanoparticles, referred in the manuscript as null-NPs). Cells were then activated with thapsigargin (TG), a SERCA (sarco/endoplasmic Ca^{2+} pump) inhibitor, which induces a robust increase in $[Ca^{2+}]_i$ via Ca^{2+} influx through CRAC channels without engaging the TCR [16, 28]. We have shown previously that decorating the nanoparticles with the anti-CD45RO antibody enables the selective delivery of the cargo (Kv1.3 siRNAs or scr RNAs) to the $CD45RO^+$

Author Manuscript Author Manuscript Author Manuscript Author Manuscript

memory T cells and not CD45RA$^+$ naïve T (T_{naive}) cells [26]. CD45RO$^+$ T cells were acquired using imaging flow cytometry and we studied NFAT nuclear translocation in these cells (for analysis, see Supplemental Fig. 1). The incorporation of the NPs, which identifies CD45RO$^+$ T cells, is visible in the Ch11 channel of the images shown in Fig. 1A and B. Activated CD45RO$^+$ T cells pre-treated with scr-NPs (Fig. 1A and C) showed significant NFAT nuclear translocation (89 ± 12 % of the cells, n= 3 donors), while treatment with Kv1.3-NPs significantly reduced the NFAT translocation (41 ± 12% of cells, n= 3 donors, $p<0.001$) (Fig. 1A and C). Resting CD45RO$^+$ T cells incubated with null-NPs displayed only baseline NFAT nuclear localization (21 ± 3% of the cells, n= 3 donors, Fig. 1B and C), which was not significantly different from that of the cells with Kv1.3-NPs ($p=0.2$). Overall, our data show that Kv1.3-NPs effectively reduce NFAT nuclear accumulation in CD45RO$^+$ T cells.

NFAT activation in T cells controls the expression of CD40L. We thus investigated the effect of Kv1.3-NPs on CD40L expression in CD45RO$^+$ T cells.

3.2 Kv1.3 nanoparticles decrease CD40L expression in memory T cells

CD40L transcription in T cells was induced by activation with TG. TG induced a significant increase in CD40L levels, comparable to that produced by PMA and ionomycin, which mimic the various biochemical pathways of TCR stimulation [9, 16, 28] (Supplemental Fig. 2). Both TG and PMA/ionomycin triggered a robust increase in CD40L, superior to that induced by direct stimulation of TCR with anti-CD3/CD28 antibodies (Supplemental Fig 2). We thus performed experiments to determine if Kv1.3-NPs reduced TG-induced CD40L expression in the CD45RO$^+$ T cell population. CD3$^+$ cells were incubated overnight with Kv1.3-, scr- and null-NPs. Cells were then activated for 3 hours with TG, and CD40L expression was assessed using flow cytometry in cells that had incorporated the NPs (CD45RO$^+$ T cells) and those that did not (CD45RO$^-$ T_{naive} cells). Similar analysis was performed in resting CD3$^+$ cells transduced with null-NPs that were used as negative controls.

As shown in representative experiments presented in Fig. 2A, the percentage of CD40L$^+$ cells was reduced by 47% in activated CD45RO$^+$ T cells treated with Kv1.3-NPs as compared to activated cells that incorporated scr- and null-NPs (Fig. 2A–C). The mean fluorescence intensity (MFI) of CD40L expression in activated CD45RO$^+$ T cells transduced with Kv1.3-NPs was reduced by 52% as compared to scr-NP treated controls ($p=0.03$, n=3, Fig. 2C). The percentage of CD40L$^+$CD45RO$^+$ cells, which was normalized to the CD40L$^+$CD45RO$^+$, null-NP-treated T cell subpopulation, was reduced from 96 ± 5% in scr-NP treated cells to 58 ± 5% in siKv1.3-NP treated cells (n=3, $p<0.001$, Fig 2D). Resting cells with null-NPs had no CD40L expression (3 ± 1% CD40L$^+$CD45RO$^+$ cells, Fig 2D). Contrary to CD45RO$^+$ T cells, the CD40L expression in activated CD45RO$^-$ T cells was not altered by exposure to Kv1.3-NPs. We have previously shown that the T cells that did not pick up the CD45RO$^+$ NPs were CD45RA$^+$ T_{naive} cells [26]. As shown in Fig 2E, the percentage of CD40L$^+$CD45RO$^-$ cells in scr-NP treated cells (87 ± 8%) and Kv1.3-NP treated cells (99 ± 8%, n=3, $p=0.3$) was not significantly different. These data show both efficacy and specificity of Kv1.3-NPs. Interestingly, we observed a further benefit of Kv1.3-

Author Manuscript Author Manuscript Author Manuscript Author Manuscript

NPs: they reduce the fraction of CD45RO$^+$ T cells in the overall T cell population (compare Fig. 2A panel scr-NP and Kv1.3-NP).

3.3 Kv1.3 nanoparticles induce a shift in the phenotype of T cells

Our data indicated that incubation of a mixed population of T cells with Kv1.3-NPs decreased the percentage of CD45RO$^+$ cells and caused an increase in the CD45RO$^-$ population (Fig. 3). The CD3$^+$ mixed cell population is comprised predominantly of CD45RO$^+$ T cells as indicated by the CD45RO$^+$/CD45RO$^-$ T cell ratio of 1.4 ± 0.2 in null-NP treated cells and 1.5 ± 0.1 in scr-NP incubated cells (n=3, p=0.5 compared to null NP, Fig 3A–B). This ratio is decreased by 45% to 0.8 ± 0.0 in cells treated with Kv1.3-NPs (n=3, p<0.001 compared to null- and scr-NP, Fig. 3B). These data suggest that Kv1.3-NPs induce a shift from a predominantly CD45RO$^+$ to a predominantly CD45RO$^-$ phenotype in the T lymphocyte population.

Still, we do not know whether this effect is due to the fact that CD45RO$^+$ cells die or there is an actual loss of memory marked by the loss of CD45RO expression. To investigate whether the decrease in CD45RO is indicative of a switch from memory to naïve T cell phenotype, we isolated CD4$^+$ memory T cells from healthy donors and studied the effect of Kv1.3-NPs on CD45RO expression, cell viability and cytokine release. Memory CD4$^+$ T cells treated with Kv1.3- or scr-NPs were stained with anti-CD45RO and anti-CD45RA antibodies to quantitate the memory and naïve T cell populations, respectively. We observed that, after incubation with Kv1.3-NPs, there was a change in the phenotype of the memory CD4$^+$ T cells from predominantly CD45RO$^+$CD45RA$^-$ to predominantly CD45RO$^-$CD45RA$^-$ (Fig 4A). The percentage of CD45RO$^+$ cells decreased from 81 ± 7% in memory CD4$^+$ T cells treated with scr-NPs to 32 ± 11 % in memory CD4$^+$ T cells treated with Kv1.3-NPs (n=3, p=0.02, Fig. 4B). A commensurate reduction in the MFI of CD45RO expression was seen in Kv1.3-NP treated memory CD4$^+$ T cells (Fig. 4C). In one donor we observed that the decrease in CD45RO$^+$ cells was accompanied by an increase in CD45RA$^+$ cells (Fig. 4D). Importantly, the “switch-off” of the CD45RO phenotype was not due to loss of CD45RO$^+$ cells. The addition of Kv1.3-NPs did not induce cell death as indicated by no increase in 7-AAD$^+$ cells (Fig. 4E).

We ultimately assessed cytokine production which has been reported to be greater in T_{EM} (effector memory T cells) than T_{CM} (central memory T cells; T_{CM} cells constitute 5% of the memory T cell population) and $T_{naïve}$ cells [29]. We observed that memory CD4$^+$ T cells that were treated with Kv1.3-NPs have a significantly diminished ability to produce IFN-γ (Fig 4F, H) and TNF-α (Fig. 4G, H). IFN-γ and TNF-α expressions were reduced by 66 % and 71%, respectively (n=3), indicating that the loss of the memory marker CD45RO is accompanied by decreased effector functions (Fig. 4H). Overall, these findings show that Kv1.3-NPs effectively suppress memory and effector function of CD45RO$^+$ T cells.

4. DISCUSSION

In the present study, we have presented evidence that Kv1.3 downregulation by targeted nanoparticles in memory T cells suppresses NFAT activation, CD40L expression and cytokine production in this cell subset. These effects are accompanied by the loss of the T

Author Manuscript Author Manuscript Author Manuscript Author Manuscript

cell memory phenotype. Thus, Kv1.3-NPs may effectively correct the T cell abnormalities responsible for autoimmune disease-associated pathologies. Beforehand, our laboratory has successfully fabricated lipid nanoparticles that were decorated with CD45RO antibodies.

We have shown that these NPs can deliver siRNAs against Kv1.3 channels and effectively knocked down the channels in the $CD45RO^+$ T cell population [26]. We have also demonstrated that downregulation of Kv1.3 channels by these NPs prevents Ca^{2+} influx, an early event during T cell activation, in the $CD45RO^+$ T cell sub-population [26]. In the present manuscript we have evaluated the consequences of Kv1.3 channel inhibition by Kv1.3-NPs on the downstream effects of Ca^{2+} influx in activating T cells: NFAT translocation, expression of CD40L and production of cytokines. Although selective inhibition of Kv1.3 channels by Kv1.3 antagonist has been shown to ameliorate autoimmune diseases, the potentials for selective nanoparticle-based Kv1.3 blockade as therapy for autoimmunity is largely unexplored [6, 23, 30]. The data presented herein show that Kv1.3-NPs suppress NFAT nuclear translocation. This effect is very important in the treatment of autoimmunity as inhibition of the NFAT pathway is the main target of effective immunosuppressive agents like cyclosporine and tacrolimus [17].

Furthermore, NFAT regulates CD40L expression of T cells, and its interaction with CD40 on B cells and DCs constitutes an important pathway by which T cells (re-)activate both of these cells. In parallel with increased NFAT nuclear translocation, the surface expression of CD40L in SLE T cells is higher than in their healthy counterparts [31]. Thus, the CD40-CD40L interaction is particularly troublesome in SLE patients where the CD40-CD40L interaction contributes the hyperactivity of B cells/DCs, all involved in the pathology of SLE [1, 32]. A recent study by Shaw et al reported that CD40L expression in human T cells is explicitly linked to Ca^{2+} influx through CRAC channels [33]. In agreement with this, we reported that CD40L expression is upregulated upon the inhibition of SERCA pump by TG, which induces the assembly of Orai1-STIM complex and the influx of Ca^{2+} through these channels due to the emptying ER Ca^{2+} stores. Also, we could show that the increase in CD40L expression during T cell activation could be remarkably abrogated by Kv1.3-NPs. The inhibition of CD40L by Kv1.3-NPs is consistent with studies showing that CD40L increased expression in SLE T cells is reduced by suppression of Ca^{2+} influx with inhibitors such as cyclosporine, especially when they are added at the early stages of stimulation [1, 6, 7, 34]. Since the effect of Kv1.3-NPs is observed when T cells are stimulated with TG, this indicates that suppressing Ca^{2+} influx is sufficient to downregulate CD40L expression in T cells.

The data we reported here also suggest that Kv1.3-NPs may induce a switch in T cell phenotype in a mixed population of human T cells from memory T cells to naïve T cells. This is indicated by the loss of CD45RO expression (which, in one donor, the loss of CD45RO expression was accompanied by an increase in CD45RA expression) in memory $CD4^+$ T cells and suppression of cytokine release. This may be an important pleiotropic effect of Kv1.3 knockdown, since memory T cells are key participants in the chronicity of autoimmune diseases. Others have shown that Kv1.3 knock-down resulted in a decrease in T_{EM} ($CCR7^-CD45RA^-$) cells and an increase in $T_{naïve}$ ($CCR7^+CD45RA^+$) and T_{CM} ($CCR7^+CD45RA^-$) cells [35]. The possibility that Kv1.3 knock-down triggers loss of

Author Manuscript Author Manuscript Author Manuscript Author Manuscript

memory is further supported by recent finding showing that CD40L as well as Ca^{2+} influx via CRAC channels are necessary for maintenance of memory in $CD8^+$ cells [33, 36]. Specifically, Shaw et al. have shown by means of the STIM1/$STIM2^{-/-}$ mice model that CRAC channels control the maintenance of virus-specific memory $CD8^+$ cells and their ability to mediate recall responses to secondary infections [33]. In this model, the defective maintenance of memory $CD8^+$ T cells has been attributed to reduced CD40L expression in $CD4^+$ cells which is known to be critical for DC activation and production of virus-specific antibody. Similarly, it is plausible to speculate that the Kv1.3-NPs will act as effective immunosuppressive agents by reducing the CD40L expression in autoreactive memory T cells, thus limiting their ability to activate B cells and DCs and, ultimately, the production of autoantibodies. This effect of the Kv1.3-NPs upstream to B cells would strengthen their therapeutic efficacy in autoimmunity and it is an advantage over available treatments. Recently, nanogel-type particles have been successfully used in a lupus mouse model to selectively inhibit calmodulin-dependent protein kinases in $CD4^+$ T cells. This treatment has been shown to decrease IL-17 production and reduce proteinuria in the model animals. However, it did not reduce the titers of anti-DNA antibodies assuming that the treatment modality has no effect on autoreactive B cells [37].

The effect of the $CD45RO^+$ Kv1.3-NPs we developed is, within a T cell mixed population, specific to $CD45RO^+$ T cells as no endocytosis of the NPs was detected for $CD45RA^+$ T_{naive} cells [26]. Still, other $CD45RO^+$ cells may bind these NPs: macrophages, a subset of B cells and DCs express CD45RO as well as Kv1.3 channels, which are involved in their function [38–40]. Kv1.3 controls proliferation and inducible nitric oxide synthase (iNOS) expression in macrophages, while it regulates the expression of co-stimulatory molecules, including CD40 and CD80, in DCs [36]. In B cells Kv1.3 blockers suppress proliferation of class-switched memory B cells and, presumably, plasma cells but it may not affect primary and memory antibody response as these functions do not require Ca^{2+} influx through CRAC channels [36]. The Kv1.3-NPs may suppress antibody production indirectly, by limiting CD40L- and BAFF-mediated B cell stimulation. Overall, the potential direct effects of Kv1.3-NPs on macrophages, B cells and DCs could be of further advantage in the treatment of autoimmunity and, particularly, SLE where these cells have been implicated in its pathology. Further studies are necessary to identifying the effect of Kv1.3-NPs on other immune cells.

In conclusion, herein, we are proposing a nanoparticle-based therapy for autoimmunity targeting Kv1.3 channels in $CD45RO^+$ cells. The advantage of such therapy over existing pharmacological Kv1.3 blockers is that it may have limited side effects as $CD45RO^-$ $Kv1.3^+$ cells like naïve T cells, non-hematopoietic cells like adipose cells and olfactory neurons, and platelets are excluded. The exclusion of the latter is important to avoid thrombolytic complications. Furthermore, the nanoparticles that we have developed constitute a “versatile” platform that can be easily tailored to deliver drugs/inhibitors and siRNAs, and can be easily decorated with antibodies and protein aptamers against any target of interest [26]. In addition, because of their composition (they are nano-liposomes of natural lipids) and their targeted delivery, they may present a high safety profile. Similar lipid NPs have shown no toxicity in vivo [41, 42]. Eventually, in vivo studies will be established to test the efficacy of these NPs. While the difference in Kv channel expression in mouse T cells

Author Manuscript Author Manuscript Author Manuscript Author Manuscript

compared to human T cells limits the experimental models available, the development of humanized mice will provide the appropriate setting for studying Kv1.3-targeting NPs in vivo [20, 43].

Supplementary Material

Refer to Web version on PubMed Central for supplementary material.

Acknowledgments

This project was funded in part by NIH grants R21AR060966, R01CA095286 and a research grant from Dialysis Clinic, Inc. to LC. All flow cytometry experiments were performed at the Research Flow Cytometry Core in the Division of Rheumatology at Cincinnati Children's Hospital Medical Center and Shriner's Hospital for Children Flow Cytometry Core, Cincinnati OH. We thank Dr. Heather Duncan for her assistance with IRB regulatory affairs and Dr. Giovanni Pauletti for making the Zetasizer Nano ZS instrument available to us. We are also grateful to Dr. Judith Heiny and Dr. Christy Holland for the use of the lyophilizer. All authors discussed the results and commented on the manuscript.

References

1. Crispin JC, Kyttaris VC, Terhorst C, Tsokos GC. T cells as therapeutic targets in SLE. Nat Rev Rheumatol. 2010; 6:317–25. [PubMed: 20458333]
2. Peters AL, Stunz LL, Bishop GA. CD40 and autoimmunity: The dark side of a great activator. Seminars in Immunology. 2009; 21:293–300. [PubMed: 19595612]
3. Yoo S-A, Park B-H, Park G-S, Koh H-S, Lee M-S, Ryu SH, et al. Calcineurin Is Expressed and Plays a Critical Role in Inflammatory Arthritis. The Journal of Immunology. 2006; 177:2681–90. [PubMed: 16888030]
4. Senhaji N, Kojok K, Fadainia C, Darif Y, Zaid Y. The contribution of CD40/CD40L axis in inflammatory bowel disease: an update. Frontiers in Immunology. 2015; 6
5. Schwarz A, Tutsch E, Ludwig B, Schwarz EC, Stallmach A, Hoth M. Ca2+ Signaling in Identified T-lymphocytes from Human Intestinal Mucosa: RELATION TO HYPOREACTIVITY, PROLIFERATION, AND INFLAMMATORY BOWEL DISEASE. Journal of Biological Chemistry. 2004; 279:5641–7. [PubMed: 14585840]
6. Kyttaris VC, Wang Y, Juang Y-T, Weinstein A, Tsokos GC. Increased Levels of NF-ATc2 Differentially Regulate CD154 and IL-2 Genes in T Cells from Patients with Systemic Lupus Erythematosus. The Journal of Immunology. 2007; 178:1960–6. [PubMed: 17237447]
7. Kyttaris VC, Zhang Z, Kampagianni O, Tsokos GC. Calcium signaling in systemic lupus erythematosus T cells: A treatment target. Arthritis & Rheumatism. 2011; 63:2058–66. [PubMed: 21437870]
8. Desai-Mehta A, Lu L, Ramsey-Goldman R, Datta SK. Hyperexpression of CD40 ligand by B and T cells in human lupus and its role in pathogenic autoantibody production. J Clin Invest. 1996; 97:2063–73. [PubMed: 8621796]
9. Koshy M, Berger D, Crow MK. Increased expression of CD40 ligand on systemic lupus erythematosus lymphocytes. J Clin Invest. 1996; 98:826–37. [PubMed: 8698875]
10. Ramanujam M, Davidson A. Targeting of the immune system in systemic lupus erythematosus. Expert Rev Mol Med. 2008; 10:e2. [PubMed: 18205972]
11. Toubi E, Shoenfeld Y. The Role of CD40–CD154 Interactions in Autoimmunity and the Benefit of Disrupting this Pathway. Autoimmunity. 2004; 37:457–64. [PubMed: 15621572]
12. Yazdany J, Davis J. The role of CD40 ligand in systemic lupus erythematosus. Lupus. 2004; 13:377–80. [PubMed: 15230296]
13. Chan VS-F, Nie Y-J, Shen N, Yan S, Mok M-Y, Lau C-S. Distinct roles of myeloid and plasmacytoid dendritic cells in systemic lupus erythematosus. Autoimmunity Reviews. 2012; 11:890–7. [PubMed: 22503660]

Author Manuscript Author Manuscript Author Manuscript Author Manuscript

14. Vincent FB, Morand EF, Schneider P, Mackay F. The BAFF/APRIL system in SLE pathogenesis. Nat Rev Rheumatol. 2014 advance online publication.
15. Senhaji N, Kojok K, Darif Y, Fadainia C, Zaid Y. The Contribution of CD40/CD40L Axis in Inflammatory Bowel Disease: An Update. Frontiers in Immunology. 2015; 6:529. [PubMed: 26528290]
16. Gwack Y, Feske S, Srikanth S, Hogan PG, Rao A. Signalling to transcription: Store-operated Ca2+ entry and NFAT activation in lymphocytes. Cell Calcium. 2007; 42:145–56. [PubMed: 17572487]
17. Hogan PG, Chen L, Nardone J, Rao A. Transcriptional regulation by calcium, calcineurin, and NFAT. Genes Dev. 2003; 17:2205–32. [PubMed: 12975316]
18. Clipstone NA, Crabtree GR. Identification of calcineurin as a key signalling enzyme in T-lymphocyte activation. Nature. 1992; 357:695–7. [PubMed: 1377362]
19. Tenbrock K, Juang Y-T, Kyttaris VC, Tsokos GC. Altered signal transduction in SLE T cells. Rheumatology. 2007; 46:1525–30. [PubMed: 17586862]
20. Cahalan MD, Chandy KG. The functional network of ion channels in T lymphocytes. Immunological Reviews. 2009; 231:59–87. [PubMed: 19754890]
21. Nicolaou SA, Szigligeti P, Neumeier L, Molleran Lee S, Duncan HJ, Kant SK, et al. Altered Dynamics of Kv1.3 Channel Compartmentalization in the Immunological Synapse in Systemic Lupus Erythematosus. The Journal of Immunology. 2007; 179:346–56. [PubMed: 17579055]
22. George Chandy K, Wulff H, Beeton C, Pennington M, Gutman GA, Cahalan MD. K+ channels as targets for specific immunomodulation. Trends in Pharmacological Sciences. 2004; 25:280–9. [PubMed: 15120495]
23. Beeton C, Wulff H, Barbaria J, Clot-Faybesse O, Pennington M, Bernard D, et al. Selective blockade of T lymphocyte K+ channels ameliorates experimental autoimmune encephalomyelitis, a model for multiple sclerosis. Proceedings of the National Academy of Sciences. 2001; 98:13942–7.
24. Lam J, Wulff H. The lymphocyte potassium channels Kv1.3 and KCa3.1 as targets for immunosuppression. Drug Development Research. 2011; 72:573–84. [PubMed: 22241939]
25. Lo MS, Tsokos GC. Treatment of systemic lupus erythematosus: new advances in targeted therapy. Annals of the New York Academy of Sciences. 2012; 1247:138–52. [PubMed: 22236448]
26. Hajdu P, Chimote AA, Thompson TH, Koo Y, Yun Y, Conforti L. Functionalized liposomes loaded with siRNAs targeting ion channels in effector memory T cells as a potential therapy for autoimmunity. Biomaterials. 2013; 34:10249–57. [PubMed: 24075407]
27. Fan W, Liang D, Tang Y, Qu B, Cui H, Luo X, et al. Identification of microRNA-31 as a novel regulator contributing to impaired interleukin-2 production in T cells from patients with systemic lupus erythematosus. Arthritis & Rheumatism. 2012; 64:3715–25. [PubMed: 22736314]
28. Treiman M, Caspersen C, Christensen SB. A tool coming of age: thapsigargin as an inhibitor of sarco-endoplasmic reticulum Ca2+-ATPases. Trends in Pharmacological Sciences. 1998; 19:131–5. [PubMed: 9612087]
29. Sallusto F, Lenig D, Forster R, Lipp M, Lanzavecchia A. Two subsets of memory T lymphocytes with distinct homing potentials and effector functions. Nature. 1999; 401:708–12. [PubMed: 10537110]
30. Beeton C, Pennington MW, Wulff H, Singh S, Nugent D, Crossley G, et al. Targeting Effector Memory T Cells with a Selective Peptide Inhibitor of Kv1.3 Channels for Therapy of Autoimmune Diseases. Molecular Pharmacology. 2005; 67:1369–81. [PubMed: 15665253]
31. Tsokos GC. Systemic Lupus Erythematosus. New England Journal of Medicine. 2011; 365:2110–21. [PubMed: 22129255]
32. Kyttaris VC, Wang Y, Juang YT, Weinstein A, Tsokos GC. Increased levels of NF-ATc2 differentially regulate CD154 and IL-2 genes in T cells from patients with systemic lupus erythematosus. J Immunol. 2007; 178:1960–6. [PubMed: 17237447]
33. Shaw PJ, Weidinger C, Vaeth M, Luethy K, Kaech SM, Feske S. CD4+ and CD8+ T cell–dependent antiviral immunity requires STIM1 and STIM2. J Clin Invest. 124:4549–63. [PubMed: 25157823]
34. Mehta J, Genin A, Brunner M, Scalzi LV, Mishra N, Beukelman T, et al. Prolonged expression of CD154 on CD4 T cells from pediatric lupus patients correlates with increased CD154

Author Manuscript Author Manuscript Author Manuscript Author Manuscript

transcription, increased nuclear factor of activated T cell activity, and glomerulonephritis. Arthritis & Rheumatism. 2010; 62:2499–509. [PubMed: 20506525]

35. Hu L, Wang T, Gocke AR, Nath A, Zhang H, Margolick JB, et al. Blockade of Kv1.3 Potassium Channels Inhibits Differentiation and Granzyme B Secretion of Human CD8+ T Effector Memory Lymphocytes. PLoS One. 2013; 8:e54267. [PubMed: 23382885]
36. Feske S, Wulff H, Skolnik EY. Ion Channels in Innate and Adaptive Immunity. Annual Review of Immunology. 2015; 33:291–353.
37. Otomo K, Koga T, Mizui M, Yoshida N, Kriegel C, Bickerton S, et al. Cutting Edge: Nanogel-Based Delivery of an Inhibitor of CaMK4 to CD4+ T Cells Suppresses Experimental Autoimmune Encephalomyelitis and Lupus-like Disease in Mice. The Journal of Immunology. 2015; 195:5533–7. [PubMed: 26561550]
38. Vicente R, Escalada A, Coma M, Fuster G, Sanchez-Tillo E, Lopez-Iglesias C, et al. Differential voltage-dependent K+ channel responses during proliferation and activation in macrophages. J Biol Chem. 2003; 278:46307–20. [PubMed: 12923194]
39. Vallejo-Gracia A, Bielanska J, Hernandez-Losa J, Castellvi J, Ruiz-Marcellan MC, Ramon y Cajal S, et al. Emerging role for the voltage-dependent K+ channel Kv1.5 in B-lymphocyte physiology: expression associated with human lymphoma malignancy. J Leukoc Biol. 2013; 94:779–89. [PubMed: 23847097]
40. Deane DL, Harvey E, Steel CM. Differential effects of CD45 CD45R and CD45R0 monoclonal antibodies in modulating human B cell activation. Clin Exp Immunol. 1991; 83:175–81. [PubMed: 1703055]
41. Look M, Stern E, Wang QA, DiPlacido LD, Kashgarian M, Craft J, et al. Nanogel-based delivery of mycophenolic acid ameliorates systemic lupus erythematosus in mice. J Clin Invest. 2013; 123:1741–9. [PubMed: 23454752]
42. Peer D, Park EJ, Morishita Y, Carman CV, Shimaoka M. Systemic Leukocyte-Directed siRNA Delivery Revealing Cyclin D1 as an Anti-Inflammatory Target. Science. 2008; 319:627–30. [PubMed: 18239128]
43. Beeton C, Chandy KG. Potassium Channels, Memory T Cells, and Multiple Sclerosis. The Neuroscientist. 2005; 11:550–62. [PubMed: 16282596]

Author Manuscript Author Manuscript Author Manuscript Author Manuscript

Highlights

- Nanoparticles that selectively silence Kv1.3 channels in memory T cells were used
- Nanoparticles selectively reduced CD40 ligand expression in memory T cells
- Nanoparticles reduced number of memory T cells
- Promising therapeutic potential for Kv1.3 silencing in autoimmune diseases

Author Manuscript Author Manuscript Author Manuscript Author Manuscript

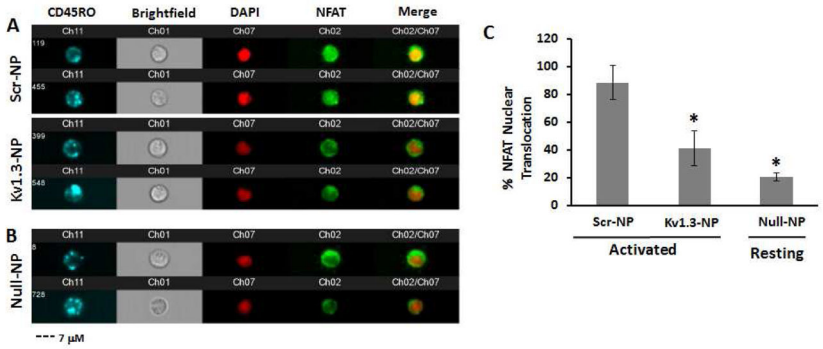

Figure 1. Kv1.3 nanoparticles decrease NFAT nuclear translocation in CD45RO$^+$ T cells

CD3$^+$ cells were incubated overnight with Alexa 647 anti-CD45RO coated NPs that contained either Kv1.3 siRNA (Kv1.3-NPs), scramble sequence RNA (scr-NPs) or neither (null-NPs). Cells were then activated for 1 h with TG, permeabilized and stained with Alexa-488 anti-NFAT antibody, while nuclei were stained with DAPI. Quantitative imaging flow cytometry was used to measure nuclear translocation. Only cells that expressed Alexa 647 fluorescence (CD45RO$^+$ T cells) were acquired. The gating strategies for image acquisition are described in Supplemental Figure 1 and Methods section (Section 2.6). **A–B)** Representative images of CD3$^+$ cells acquired by imaging flow cytometry. Shown are TG-activated cells, which took up scr-NPs (top) or Kv1.3-NPs (bottom) **(A)** and resting T cells treated with null-NPs **(B)**. The NPs are visualized as blue fluorescence in Ch11 (Alexa 647 fluorophore conjugated SAV was used in the fabrication of the NPs), DAPI as red fluorescence in Ch07 and NFAT as green fluorescence in Ch02 (Alexa488 anti-NFAT antibody). The nuclear translocation of NFAT in activated CD45RO$^+$ T cells is indicated by the colocalization of red and green channels in the merged images (column Ch02/Ch07). **(C)** Percentage nuclear translocation of NFAT in activated T cells treated with scr- or Kv1.3-NPs or resting T cells with null-NPs. The data are normalized to activated null-NPs (considered as 100% translocation) and are presented as mean ± SEM for 3 donors, with 2300–3500 cells recorded per donor. Scale Bar = 7 µm. * indicates statistical significance $p<0.05$ compared to scr-NPs.

Author Manuscript Author Manuscript Author Manuscript Author Manuscript

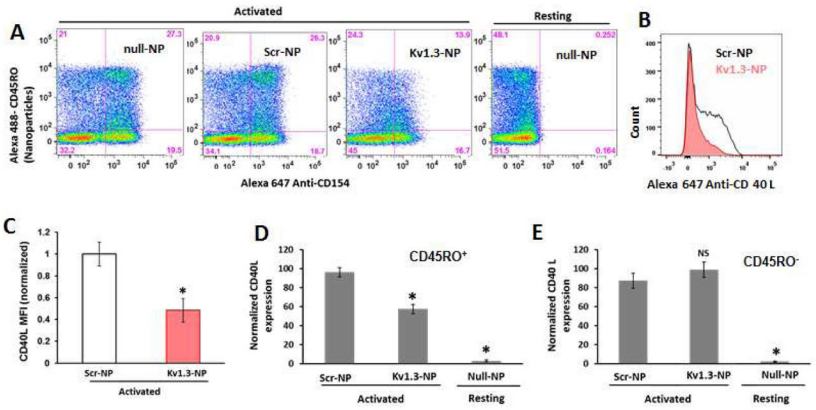

Figure 2. Kv1.3 nanoparticles decrease CD40L expression in CD45RO$^+$ T cells

(A) Representative scatter plots for CD40L expression as a function of CD45RO expression in activated (TG addition, 3 hours) or resting CD3$^+$ cells. Cells were incubated overnight with null-NPs, scr-NPs or Kv1.3-NPs (Alexa488 SAV was used for functionalization) as displayed on each panel. The fluorescence intensity of Alexa647 (CD40L) and Alexa488 (NP-targeted CD45RO$^+$ T cells) was detected in each cell. Quadrant gates were drawn based on cells without NPs and stained with the isotype control antibody and the numbers in each quadrant correspond to the percentage of cells. **(B)** Histogram of CD40L expression in activated CD45RO$^+$ CD3$^+$ cells treated with scr-NPs (black line) or Kv1.3-NPs (red line). Representative experiment from n=3 donors. **(C)** Average mean fluorescence intensity (MFI) of CD40L expression in activated, scr-NPs or Kv1.3-NPs treated CD3$^+$ cells (n=3 donors). Data normalized to MFI of scr-NPs. **(DE)** Average CD40L expression in NP$^+$ (CD45RO$^+$ T**, D**) or NP$^-$ (CD45RO$^-$ T cells, **E**) cells. Cells were treated with scr-NP, Kv1.3-NPs or null-NPs. Values are normalized to activated null-NPs. Data are shown as mean ± SEM for 3 donors, with 20,000–50,000 total cells recorded in each sample. * = statistically significant difference, NS: no statistical significance, both compared to scr-NPs (p values given in section 3.2).

Author Manuscript Author Manuscript Author Manuscript Author Manuscript

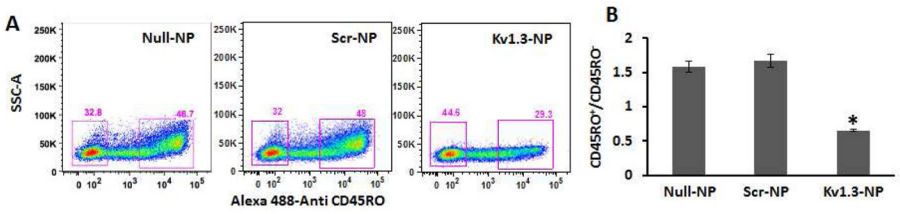

Figure 3. Kv1.3 nanoparticles induce loss of CD45RO expression

(A) Representative flow cytometry dot plots for CD45RO expression in $CD3^+$ cells from a donor preincubated with null-, scr- or Kv1.3-NPs overnight and then activated with TG for 3 h. CD45RO expression was plotted as function of side scatter (SSC-A). $CD45RO^+$ memory T and $CD45RO^-$ naïve T cell populations were selected by drawing rectangle gates. The numbers next to the gates are the percentages of $CD45RO^+$ and $CD45RO^-$ cells. **(B)** Ratio of $CD45RO^+/CD45RO^-$ activated $CD3^+$ cells treated with null-, scr- or Kv1.3-NPs. Data show mean ± SEM (3 donors), with 20,000 total cells recorded in each experiment. *: statistically significant difference as compared to null-NPs treated sample, p values given in section 3.3.

Author Manuscript Author Manuscript Author Manuscript Author Manuscript

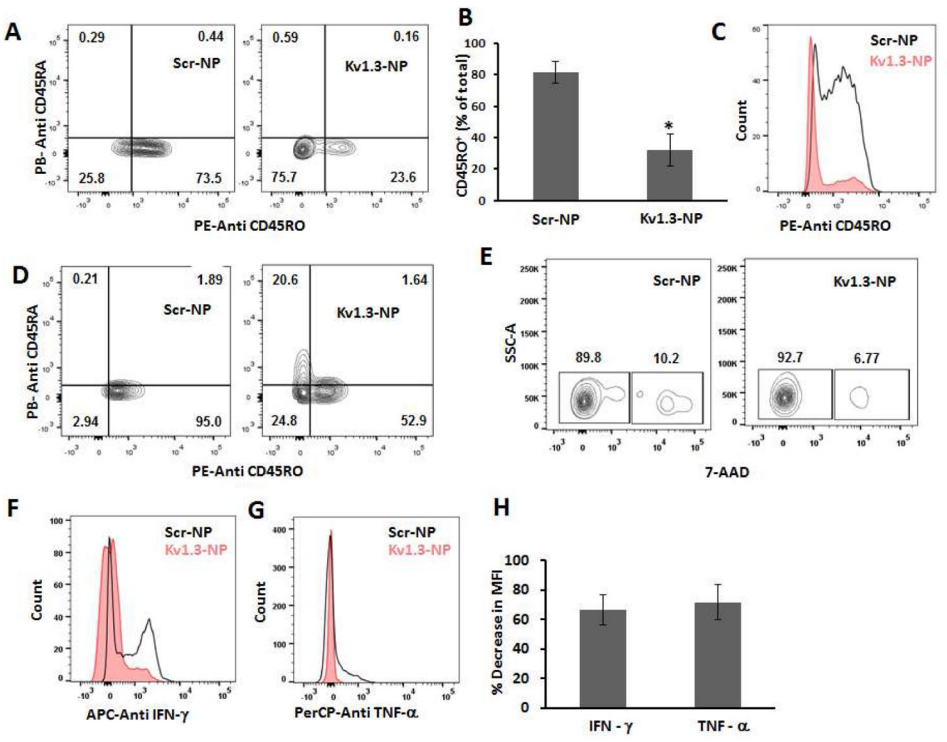

Figure 4. Kv1.3-NPs reduce CD45RO expression and cytokine levels in memory CD4$^+$ T cells

(A) Representative flow cytometry contour plots for CD45RO and CD45RA expression in memory CD4$^+$ T cells incubated with scr- or Kv1.3-NPs and then activated with PMA/ionomycin for 3 h. Populations were identified by drawing quadrant gates and the numbers in the gates are the percentages of cells in the quadrant. Shown here is a representative experiment. **(B)** CD45RO expression was measured as the percentage of CD45RO$^+$ cells out of total cells treated with scr-NP or Kv1.3-NP (n=3). Data are mean ± SEM, 20,000 were cells recorded in each sample. *: statistically significant difference (p-values are given in the results section). **(C)** Representative histograms of CD45RO expression in activated memory CD4$^+$ T cells treated with scr-NP (black line) or Kv1.3-NPs (red line). **(D)** Flow cytometry contour plots for CD45RO and CD45RA expression in memory CD4$^+$ T cells isolated from a single donor and incubated with either scr- or Kv1.3-NPs and then activated with PMA/ionomycin for 3 h. Please note the increase in CD45RA$^+$ cells in Kv1.3-NP treated cells (right panel) **(E)** Viability for memory CD4$^+$ T cells shown in (A) was measured by flow cytometry using the nuclear dye 7-AAD for a representative donor. 7-AAD fluorescence was plotted as a function of side scatter (SSC-A). Rectangle gates were drawn to identify the 7-AAD$^+$ (non-viable/dead) and 7-AAD$^-$ (live) cell populations and the numbers above the gates are the percentages of 7-AAD$^+$ and 7-AAD$^-$ cell populations. **(F)** Representative histogram of IFN-γ expression in activated memory CD4$^+$ T cells from a representative donor treated with scr-NP or Kv1.3-NPs. **(G)** Typical histogram of TNF-α expression in activated memory CD4$^+$ T cells preincubated with scr-NP or Kv1.3-NPs. **(H)** Decrease in IFN-γ and TNF-α expression in Kv1.3-NPs pre-treated memory CD4$^+$ T cells expressed as

the percentage of MFI values normalized to scr-NP treated controls. Data are presented as mean ± SEM for 3 donors with 20,000 cells recorded for each sample.

Author Manuscript Author Manuscript Author Manuscript Author Manuscript